

Pericyclic and Pseudopericyclic Thermal Cheletropic Decarbonylations: When Can a Pericyclic Reaction Have a Planar, Pseudopericyclic Transition State?¹

David M. Birney,* Sihyun Ham, and Gregory R. Unruh[†]

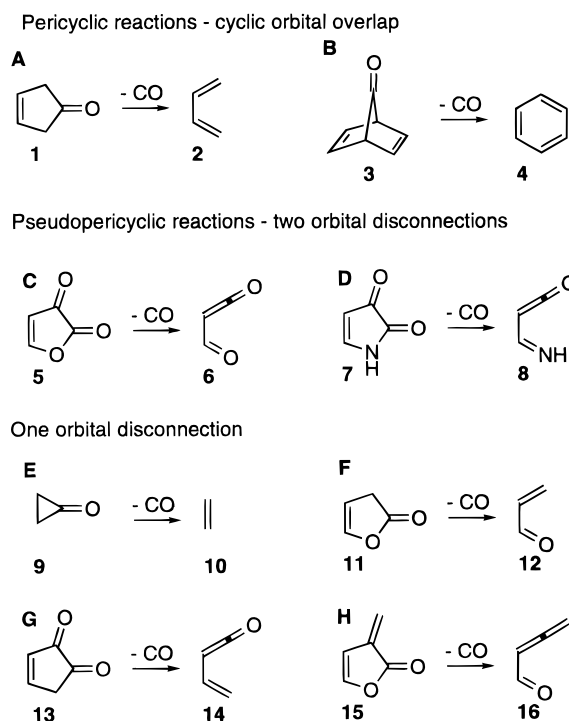
Contribution from the Department of Chemistry and Biochemistry, Texas Tech University, Lubbock, Texas 79409-1061

Received October 11, 1996. Revised Manuscript Received March 14, 1997[⊗]

Abstract: A series of eight thermal cheletropic decarbonylations show dramatic differences in reaction pathways and in activation energies depending on the molecular orbital topology, as calculated by using *ab initio* molecular orbital theory (MP2(FC)/6-31G* optimized geometries and MP4/D95** + ZPE single point energies). The decarbonylations of 3-cyclopentenone (**1**) and bicyclo[2.2.1]hepta-2,5-diene-7-one (**3**) are pericyclic, orbital symmetry allowed reactions, but it is argued that the decarbonylation of cyclopropanone (**9**), although formally orbital symmetry allowed, lacks an energy of concert and thus is “effectively forbidden”. The carbon monoxide produced from **1** is predicted to be formed vibrationally cool and rotationally hot. Fragmentations of 2,3-furandione (**5**) and 2,3-pyrroledione (**7**) are pseudopericyclic reactions with two orbital disconnections, proceed via planar transition structures, and have activation energies that are much lower than expected for pericyclic reactions of comparable exothermicity. It will be an experimental challenge to determine if the carbon monoxide product from each of these is formed with little vibrational or rotational excitation as predicted. Fragmentations of 3*H*-furan-2-one (**11**), 3-cyclopentene-1,2-dione (**13**), and 3-methylene-3*H*-furan-2-one (**15**) each have a single disconnection. Strong bonding at the orbital disconnection in the transition structure tends to lower the barrier and give the reaction more pseudopericyclic character.

Pericyclic reactions were originally defined as “reactions in which all first-order changes in bonding relationships take place in concert on a closed curve”.² In addition, for *most, but not all*, pericyclic reactions, the orbitals involved in bonding changes also overlap in a closed loop.³ The subset of pericyclic reactions for which there is not cyclic orbital overlap were described by Lemal as pseudopericyclic reactions.^{4,5} Two thermal decarbonylations highlight the differences between the two orbital topologies. Decarbonylation of 3-cyclopentenone (**1**, Scheme 1A) is a typical allowed pericyclic reaction. Although the ground state of **1** is planar (C_{2v} symmetry),⁷ the requirement for orbital overlap at the transition state (ITS) was predicted by Woodward and Hoffmann² to result in the departure of the CO out of the butadiene plane (Figure 1A) via an orbital symmetry allowed, disrotatory pathway with C_s symmetry.⁸ In contrast, for the decarbonylation of furandione (**5**, Scheme 1C), a pseudopericyclic orbital topology is possible, with two orbital

Scheme 1



[†] Current address: Tech Spray, Inc., P.O. Box 949, Amarillo, TX 79105-0949.

[⊗] Abstract published in *Advance ACS Abstracts*, May 1, 1997.

(1) Portions of this work were previously reported. Sihyun Ham, David M. Birney, Pacificchem, 1995, Honolulu, Hawaii.

(2) Woodward, R. B.; Hoffmann, R. *The Conservation of Orbital Symmetry*; Verlag Chemie, GmbH: Weinheim, 1970.

(3) Lowry, T. H.; Richardson, K. S. *Mechanism and Theory in Organic Chemistry*, 3rd ed.; Harper and Row, Publishers: New York, 1987; p 839.

(4) Ross, J. A.; Seiders, R. P.; Lemal, D. M. *J. Am. Chem. Soc.* **1976**, *98*, 4325–4327.

(5) Later, Wentrup independently recognized that an orbital “orthogonality”, as he termed it, could make an allowed reaction forbidden.⁶

(6) Wentrup, C.; Netsch, K. P. *Angew. Chem., Int. Ed. Engl.* **1984**, *23*, 802.

(7) Bevan, J. W.; Legon, A. C. *J. Chem. Soc., Faraday Trans. 2* **1973**, *69*, 902–925.

(8) An orbital symmetry correlation diagram is found in the Ph.D. Thesis of D. M. Birney, Yale University, 1987. The C_s pathway is also predicted by an OCAMS analysis.⁹

(9) Halevi, E. A. *Orbital Symmetry and Reaction Mechanism. The OCAMS View.*, 1st ed.; Springer-Verlag: New York, 1992.

disconnections, i.e. two atoms where orthogonal sets of orbitals meet, but do not overlap (Figure 1B). Because no electrons are exchanged between the in-plane and out-of-plane orbitals, the transition state for decarbonylation of **5** is orbital symmetry allowed when the CO departs in the plane of the molecule.¹⁰

(10) Planar transition states are neither predicted² nor calculated¹¹ for hydrocarbon pericyclic reactions, as a direct consequence of the need for cyclic orbital overlap.

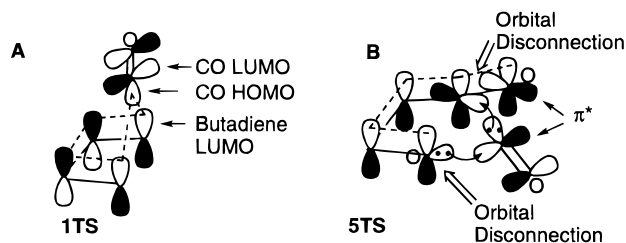


Figure 1. (A) Orbital interactions in the pericyclic decarbonylation of **1TS**. The CO is above the butadiene plane. There is cyclic orbital overlap around the ring of interacting atoms. (B) Orbital interactions in the pseudopericyclic decarbonylation of **5TS**. All the atoms are coplanar. In contrast to part A, there are orbital disconnections where the out-of-plane (arbitrary phases) and in-plane sets of orbitals meet at a single atom, but do not overlap. In both figures, the departing CO is drawn hybridized as carbon monoxide, with the carbon lone pair and one π^* orbital shown.

Just as a closed loop of interacting orbitals has dramatic chemical consequences,² so too the lack of orbital overlap in a pseudopericyclic reaction has consequences that have only recently become apparent.^{4,6,12} Previous calculations from this laboratory on a variety of thermal pseudopericyclic reactions, including cycloadditions,^{12a-d,f} sigmatropic rearrangements,^{12d,e} and electrocyclizations,^{12a,e} have led to the following generalizations:

(1) A pseudopericyclic reaction may be orbital symmetry allowed via a pathway that maintains the orbital disconnections, regardless of the number of electrons involved.^{12e,13}

(2) Barriers to pseudopericyclic reactions can be very low,^{12a} or even nonexistent¹⁶ (a) if there is a good match between nucleophilic and electrophilic sites in reactants^{12a,c,d} and (b) if the geometrical constraints of the system allow for appropriate angles in the transition state,^{12e} in close analogy to Baldwin's rules,¹⁷ and (c) if the reaction is exothermic.^{12a}

(3) Pseudopericyclic reactions will have planar transition states if possible.¹⁸ However, crowding at the transition state can lead to small distortions from planarity.^{12d,20,21} This is in contrast to typical all-hydrocarbon pericyclic reactions for which

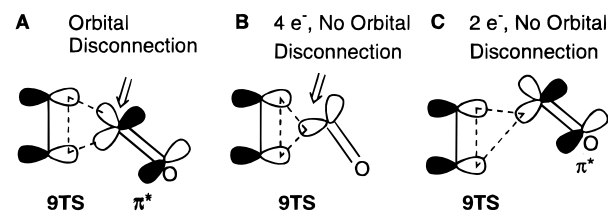


Figure 2. Possible orbital interactions in the nonlinear decarbonylation of **9**. (A) The departing CO is shown hybridized as carbon monoxide. This may be viewed as having an orbital disconnection. (B) The orbitals on the departing CO are shown sp^2 hybridized. This is an anti-aromatic, four-electron interaction. (C) The orbital interactions suggested by the calculated geometry of **9TS**. The primary interaction is between the carbon monoxide π^* orbital and the ethene π . This two-electron, aromatic interaction would give rise to the calculated offset geometry.

the need to maintain orbital overlap leads to nonplanar transition states.^{2,11}

A fundamental question regarding pseudopericyclic reactions remains unanswered; how many and what types of disconnections in the loop of interacting orbitals are necessary to obtain the energetic benefits of pseudopericyclic reaction pathway?²² In those examples reported to date from this laboratory there have been two disconnections.^{12,20} In principle, a single disconnection in the orbital overlap could be sufficient to make a reaction orbital symmetry allowed. In Lemal's original description of a pseudopericyclic reaction, the degenerate sulfoxide rearrangement of perfluorotetramethyl(Dewar thiophene *S*-oxide), there was a single disconnection.⁴ A single disconnection is also present in Woodward and Hoffmann's nonlinear pathway for the decarbonylation of cyclopropanone (Figure 2A).² However, in these systems with a single disconnection, one must consider alternative hybridization schemes²⁴ such as the sp^2 hybridization of carbon monoxide in Figure 2B. Consideration of this hybridization suggests that the nonlinear decarbonylation of **9**, although formally orbital symmetry allowed, might have a higher than expected barrier due to unfavorable HOMO–LUMO interactions and/or an anti-aromatic transition state (*vide infra*).

This question of the number and type of orbital disconnections is relevant to all the classes of pericyclic and pseudopericyclic reactions; thermal cheletropic decarbonylations²⁶ were chosen as a representative class for the systematic investigation reported here. These reactions are of fundamental interest because they are the only class of pericyclic reactions discussed by Woodward and Hoffmann in their classic monograph for which two orbital symmetry allowed pathways were proposed.² These were inappropriately designated "linear" and "nonlinear"; the "linear" decarbonylation of **1** does not occur along the molecular axis. The decarbonylations of 3-cyclopentenone (**1**) and derivatives have been extensively studied,^{7,27} including elegant measurements of the rotational and vibrational energy distributions in the extruded carbon monoxide.²⁸ Decarbonylations have long been used to generate unusual molecules and reactive intermedi-

(21) Furthermore, in one case we have shown that out-of-plane aromatic π -overlap between reactants leads not to a stabilization but to a destabilization of the planar pseudopericyclic pathway relative to a nonplanar pericyclic one, even though the latter lacks any π -aromatic stabilization.^{12c}

(22) This question was recently raised in the context of electrocyclizations of vinylallenes.²³

(23) Lopez, S.; Rodriguez, J.; Rey, J. G.; Lera, A. R. *J. Am. Chem. Soc.* **1996**, *118*, 1881–1891.

(24) For a discussion of this point in the context of Lemal's⁴ work, see ref 25.

(25) Snyder, J. P.; Halgren, T. A. *J. Am. Chem. Soc.* **1980**, *102*, 2861–2863.

(26) Mock, W. L. In *Pericyclic Reactions*; Marchand, A. P., Lehr, R. E., Eds.; Organic Reactions; Academic Press: New York, 1977; Vol. 35, Part 2, pp 141–197.

(11) Houk, K. N.; Li, Y.; Evansck, J. D. *Angew. Chem., Int. Ed. Engl.* **1992**, *31*, 682–708.

(12) (a) Birney, D. M.; Wagenseller, P. E. *J. Am. Chem. Soc.* **1994**, *116*, 6262–6270. (b) Ham, S.; Birney, D. M. *Tetrahedron Lett.* **1994**, *35*, 8113–8116. (c) Wagenseller, P. E.; Birney, D. M.; Roy, D. J. *Org. Chem.* **1995**, *60*, 2853–2859. (d) Ham, S.; Birney, D. M. *J. Org. Chem.* **1996**, *61*, 3962–3968. (e) Birney, D. M. *J. Org. Chem.* **1996**, *61*, 243–251. (f) Matsui, H.; Zuckerman, E. J.; Katagiri, N.; Sugihara, T.; Kaneko, C.; Ham, S.; Birney, D. M. *J. Phys. Chem.* In press.

(13) Cyclic overlap is explicitly considered in discussions of aromatic and/or Möbius aromatic orbital overlap.¹⁴ It is implicit in the pattern of alternating allowed and forbidden reactions predicted by the Woodward–Hoffmann rules² and Frontier Molecular Orbital theory as applied to pericyclic reactions.¹⁵ Thus these theories, while useful, are not directly applicable to pseudopericyclic reactions. Orbital symmetry arguments are more general and do not make assumptions regarding cyclic overlap.^{2,9} It is straightforward to construct an orbital correlation diagram for a planar, pseudopericyclic reaction because no electrons change from in-plane to out-of-plane orbitals from the reactant, through the transition state, to the product. Alternatively, this can be demonstrated with use of the OCAMS method.⁹

(14) (a) Zimmerman, H. E. *Acc. Chem. Res.* **1971**, *4*, 272. (b) Dewar, M. J. S. *Angew. Chem., Int. Ed. Engl.* **1971**, *10*, 761.

(15) Fukui, K. *Acc. Chem. Res.* **1971**, *4*, 57.

(16) There is no calculated barrier for the ring closure of 5-oxo-2,4-hexadienal to 2*H*-pyran-2-one.^{12e} Note that arguments based solely on orbital symmetry cannot make predictions regarding barrier heights.⁹

(17) Baldwin, J. E. *J. Chem. Soc., Chem. Commun.* **1976**, 734–736.

(18) The observation that intramolecular reactions of substituted α -oxo ketenes occur only with very long tethers is consistent with the geometric constraints of a planar transition state.¹⁹

(19) Chen, C.; Quinn, E. K.; Olmstead, M. M.; Kurth, M. J. *J. Org. Chem.* **1993**, *58*, 5011–5014.

(20) Birney, D. M. *J. Org. Chem.* **1994**, *59*, 2557–2564.

ates; recent applications include the formation of α -oxoketenes²⁹ and imidoyleketenes³⁰ (Scheme 1, parts C and D). A distinguishing characteristic of pseudopericyclic reactions is their tendency to have planar transition states. However, steric crowding in [4 + 2] reactions of formylketene and imidoyleketene leads to nonplanar distortions.^{12a,d} There should be less crowding in [4 + 1] cheletropic decarbonylations so that any distortions from planarity should reflect electronic factors rather than steric ones.

We therefore undertook this systematic *ab initio* study of thermal cheletropic decarbonylations (Scheme 1) with three goals in mind. First, this study was designed to explore the effects of zero, one, and two orbital disconnections on these reactions. Second, we sought to resolve the ambiguity in the Woodward–Hoffmann rules regarding the two allowed pathways for these reactions. Last, by examining a range of decarbonylations, we anticipated providing a more general understanding of reactivity trends. Toward these ends we have carried out *ab initio* calculations of the decarbonylations of a series of 3-cyclopentenone derivatives, as shown in Scheme 1. The level of theory used in these calculations has successfully predicted trends in reactivities of other orbital symmetry allowed reactions.^{11,31} The results of these calculations for the individual reactions will be discussed and compared with experiment when possible. The broader implications for the general understanding of pseudopericyclic reactions will also be examined.

Computational Methods

The *ab initio* molecular orbital calculations were carried out using Gaussian 92.³² Geometry optimizations were performed first at the RHF/6-31G* level and then at the MP2(FC)/6-31G* level; the latter structures are shown in Figure 3. Single-determinant wave functions such as RHF/6-31G* calculations usually qualitatively reproduce transition structures for allowed pericyclic reactions, although not for forbidden ones, while MP2 optimizations give reasonable agreement with MCSCF geometries for orbital symmetry allowed pericyclic reactions.^{11,31} Frequency calculations verified the identity of each stationary point as a minimum or transition state. Due to computer limitations it was not possible to carry out MP2(FC)/6-31G* frequency calculations on **3** or **3TS**. Selected data for optimized geometries are shown in Figure 3 and in Table 1; full geometries and vibrational frequencies are available in the Supporting Information. Point groups and the lowest or imaginary frequencies, carbonyl and ketene frequen-

cies, and dipole moments³³ for all structures are reported in Table 2. For comparison with experiment, the ketene and carbonyl frequencies could be scaled by 0.960³⁴ and 0.9427,³⁵ respectively. Mulliken charges are given in the Supporting Information.³⁶ Atom numbering is as shown in Figure 3.

Single point energies of each structure were obtained at the MP4-(FC,SDTQ)/D95** level. The double- ζ basis set, D95**, has polarization functions on all atoms.³⁸ It is significantly different from the Pople basis sets³⁹ in that the 2s and 2p coefficients are independent. This additional flexibility provides significantly lower absolute energies,^{12c} and hence is closer to the complete basis set limit, at only a modest additional computational cost. The zero-point vibrational energy (ZPE) corrections were obtained by scaling the MP2/6-31G* ZPE by 0.9646, as recommended by Pople et al.³⁴ Unless otherwise indicated, all energies discussed in the text are MP4(FC,SDTQ)/D95** with scaled ZPE corrections. Absolute energies are reported in the Supporting Information; relative energies are reported in Table 3. The calculated activation energies for the decarbonylations are shown in Figure 4 as a function of the level of theory. While the magnitudes are sensitive to the level of theory, the relative barrier heights are remarkably consistent across the levels. This supports the contention that the level of theory used in this work (MP4(FC,SDTQ)/D95**/MP2/6-31G*) is more than sufficient to calculate geometries and relative energies of transition structures for these orbital symmetry allowed reactions of neutral species.

Results and Discussion

One of the experimental criteria that has been used to identify concerted pericyclic reactions is the “energy of concert”, which implies that the barrier to a reaction is lower than it might have been because the reaction is concerted. To quantify this proposition, one may turn to the Hammond postulate⁴⁰ or the Bell–Evans–Polanyi principle,⁴¹ which suggest that for *similar* reactions, more exothermic reactions should have lower activation energies. Indeed, a very clear trend has been previously demonstrated for a wide range of orbital symmetry allowed pericyclic reactions.^{42,43} For the cheletropic decarbonylations calculated in this work, the calculated barrier heights are plotted against the heat of the reaction in Figure 5. The calculated barrier heights are in qualitative agreement with the limited experimental data available; in particular, the temperatures needed for pyrolysis of related molecules increases $5 < 7 \approx 13 < 15$.^{29,30a,44} There are clearly deviations from any single correlation; this suggests that the reactions are, in some fundamental sense, not *similar*. As will be discussed in the context of the individual cheletropic decarbonylations, the origins of these differences lie in large measure in differences in orbital topology, particularly between the pericyclic and pseudopericyclic reactions.

3-Cyclopentenone (1). Previous workers have calculated the ground state of **1** and transition states for the cheletropic

(27) (a) Lewis, J. D.; Laane, J. *Spectrochim. Acta* **1975**, *31A*, 755–763.

(b) Gordon, R. D.; Orr, D. R. *J. Mol. Spectrosc.* **1988**, *129*, 24–44. (c) Bencivenni, L.; Ramondo, F.; Quirante, J. J. *J. Mol. Struct. (Theochem)* **1995**, *330*, 389–393. (d) Quirante, J. J.; Enriquez, F. *Theor. Chim. Acta* **1994**, *89*, 251–259. (e) Rzepa, H. S. *J. Chem. Res. (S)* **1988**, 224–225. (f) Unruh, G. R. Ph.D. Thesis, Texas Tech University, 1995.

(28) (a) Simpson, C. J. S. M.; Price, J.; Holmes, G.; Adam, W.; Martin, H.-D.; Bish, S. *J. Am. Chem. Soc.* **1990**, *112*, 5089–5094. (b) Jimenez, R.; Kable, S. H.; Loison, J.-C.; Simpson, C. J. S. M.; Adam, W.; Houston, P. L. *J. Phys. Chem.* **1992**, *96*, 4188–4195. (c) Prather, K. A.; Rosenfeld, R. N. *J. Phys. Chem.* **1991**, *95*, 6544–6548.

(29) Wentrup, C.; Heilmayer, W.; Kollenz, G. *Synthesis* **1994**, 1219–1248.

(30) (a) Fulloon, B. E.; Wentrup, C. *J. Org. Chem.* **1996**, *61*, 1363–1368. (b) Fulloon, B.; El-Nabi, H. A. A.; Kollenz, G.; Wentrup, C. *Tetrahedron Lett.* **1995**, *36*, 6547–6550. (c) Kappe, C. O.; Kollenz, G.; Leung-Toung, R.; Wentrup, C. *J. Chem. Soc., Chem. Commun.* **1992**, 487–490. (d) Maslivets, A. N.; Krasnykh, O. P.; Smirnova, L. I.; Andreichikov, Y. S. *J. Org. Chem. (USSR)* **1989**, *941*–948.

(31) (a) Houk, K. N.; Gonzalez, J.; Li, Y. *Acc. Chem. Res.* **1995**, *28*, 81. (b) Jiao, H.; Schleyer, P. v. R. *Angew. Chem., Int. Ed. Engl.* **1995**, *34*, 334–337. (c) Jiao, H.; Schleyer, P. v. R. *J. Am. Chem. Soc.* **1995**, *117*, 11529–11535.

(32) Frisch, M. J.; Trucks, G. W.; Head-Gordon, M.; Gill, P. M. W.; Wong, M. W.; Foresman, J. B.; Johnson, B. G.; Schlegel, H. B.; Robb, M. A.; Replogle, E. S.; Gomperts, R.; Andres, J. L.; Raghavachari, K.; Binkley, J. S.; Gonzalez, C.; Martin, R. L.; Fox, D. J.; Defrees, D. J.; Baker, J.; Stewart, J. J. P.; Pople, J. A. In *Gaussian, Inc.: Pittsburgh, PA, 1992*.

(33) The dipole moments are consistently smaller in the transition structures, which reflects the reversed dipole moment of carbon monoxide.

(34) Kappe, C. O.; Wong, M. W.; Wentrup, C. *J. Org. Chem.* **1995**, *60*, 1686–1695.

(35) Pople, J. A.; Scott, A. P.; Wong, M. W.; Radom, L. *Isr. J. Chem.* **1993**, *33*, 345.

(36) Problems with Mulliken charges are well documented.³⁷ They are used here as a simple means to identify electrophilic and nucleophilic sites.

(37) Williams, D. E. In *Reviews in Computational Chemistry*; Boyd, D., Lipkowitz, K., Eds.; Wiley Interscience: New York, 1991; pp 219–271. (38) Dunning, T. H.; Hay, P. J. *Modern Theoretical Chemistry*; Plenum: New York, 1976.

(39) Hehre, W. J.; Radom, L.; Schleyer, P. v. R.; Pople, J. A. *Ab Initio Molecular Orbital Theory*; John Wiley and Sons: New York, 1986.

(40) Hammond, G. S. *J. Am. Chem. Soc.* **1955**, *77*, 334.

(41) (a) Bell, R. P. *Proc. R. Soc. London, Ser. A* **1936**, *154*, 414. (b) Evans, M. G.; Polanyi, M. *Trans. Faraday Soc.* **1938**, *34*, 11–29.

(42) Birney, D. M.; Berson, J. A. *Tetrahedron* **1986**, *42*, 1561–1570.

(43) In this correlation, the pericyclic loop consisted of only carbon atoms.

(44) Spangler, R. J.; Beckmann, B. G.; Kim, J. H. *J. Org. Chem.* **1977**, *42*, 2989–2996.

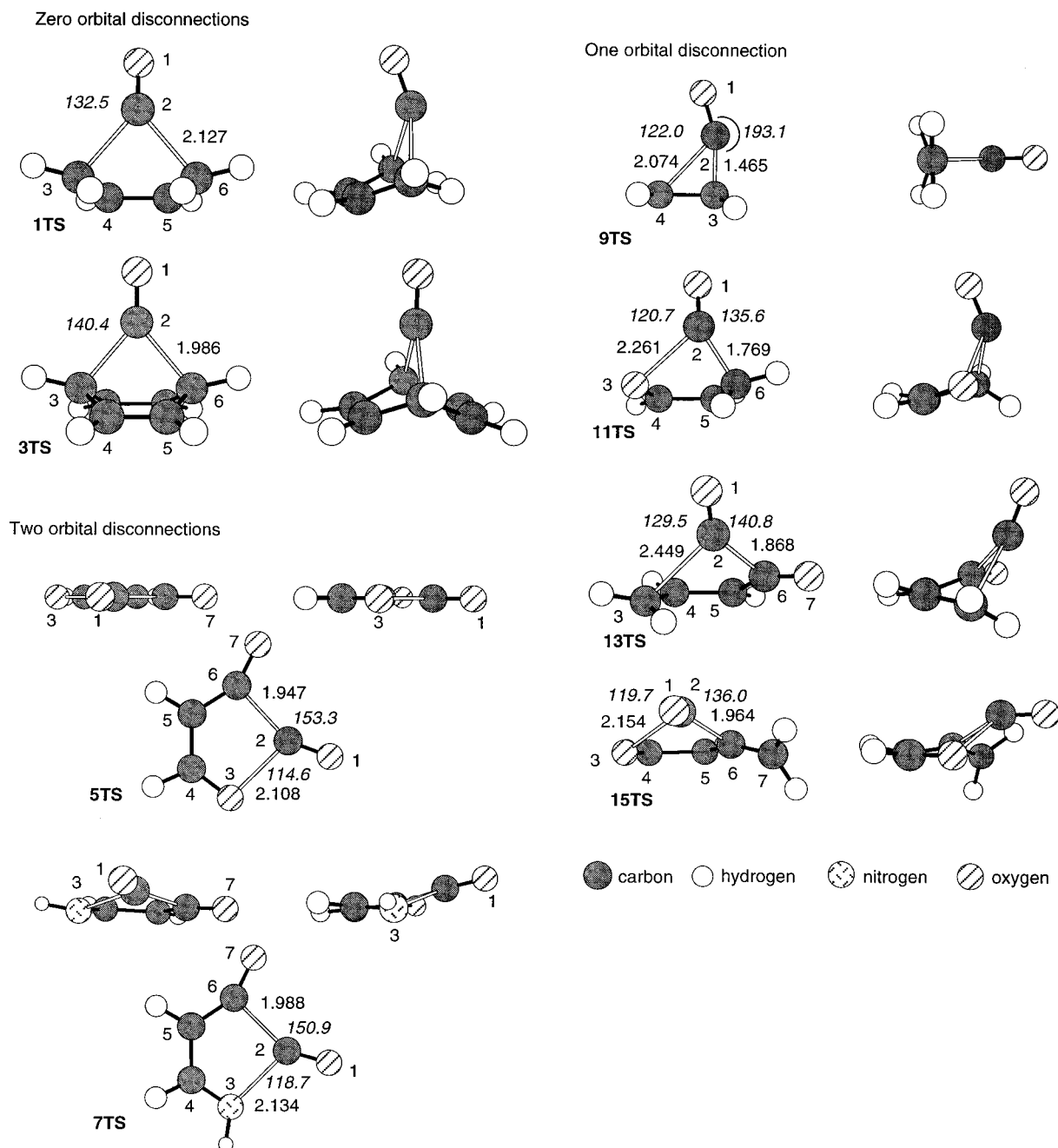


Figure 3. Transition structures optimized at the MP2/6-31G* level. Two side views, rotated by approximately 90°, are given for each structure. For 5TS and 7TS, top views are also given. Distances are in angstroms; angles are in degrees and are shown in italics.

decarbonylation of **1** at several levels of theory.^{27c-e,45} Most recently, Quirante *et al.* have reported a synchronous MP2(FU)/6-31G* transition state for this reaction.^{27c} To be consistent with the other calculations reported herein, this structure was reoptimized at the MP2(FC)/6-31G* level; this geometry, shown in Figure 3, is very similar to the MP2(FU) geometry. The

(45) Rzepa found synchronous transition states with the MNDO and AM1 semiempirical methods, as well as at the RHF/3-21G *ab initio* level.^{27c} More recently, Quirante and Enriquez reported that with the RHF/AM1 and UHF/AM1 methods, the transition state was not synchronous; they did not reference Rzepa's work.^{27d} In view of this difference, we used Gaussian92 to carry out an AM1 optimization of 1TS. The C_s symmetric structure had two imaginary frequencies, implying that the reaction is not synchronous at the AM1 level. In view of the known tendency of semiempirical calculations to erroneously predict asynchronous transition structures,^{11,46} we did not pursue this calculation further.

(46) Birney, D. M.; Wiberg, K. B.; Berson, J. A. *J. Am. Chem. Soc.* **1988**, *110*, 6631–6642.

MP4(SDTQ)/D95** single point energies calculated here have not been previously reported.

The calculated structure for **1** is in good agreement with that determined by microwave spectroscopy both in terms of bond lengths and angles and with respect to the overall planarity of the molecule (Table 1).⁷ The calculated dipole moment is slightly higher than that observed.⁷ The calculated and scaled carbonyl frequency (1815.5 cm^{-1}) is slightly higher than the observed gas-phase value of 1774 cm^{-1} .^{27a} Overall, the calculations of the ground state structure reproduce the essential features of the molecule.

Quirante *et al.* note that the geometry of the transition state and the displacements of the imaginary frequency correspond to a disrotatory motion on the butadiene fragment.^{27c} It should also be noted that the motion of the CO as it departs will give it significant rotational excitation as well as a translational

Table 1. Selected Geometrical Parameters from Structures Optimized at the MP2/6-31G* Level (distances are in Å, angles in deg)

| structure ^a | 1,2 | 2,3 | 2,6 | 3,4 | 4,5 | 5,6 | 6,7 | 1,2,3 | 1,2,6 | 5,6,7 | 1,2,3,4 | 1,2,6,5 | 4,5,6,7 | H3,3,4,5 | 3,4,5,6 |
|----------------------------|-------|-------|--------------------|-------|-------|-------|-------|-------|-------|-------|---------|---------|---------|----------|---------|
| 1 expt ^b | 1.210 | 1.524 | 1.524 | 1.509 | 1.338 | 1.509 | | 125.4 | 125.4 | | 180.0 | 180.0 | | | 0.0 |
| 1 ^c | 1.221 | 1.532 | 1.532 | 1.500 | 1.344 | 1.500 | | 125.6 | 125.6 | | 180.0 | 180.0 | | | 0.0 |
| 1TS ^c | 1.167 | 2.127 | 2.127 | 1.398 | 1.403 | 1.398 | | 132.5 | 132.5 | | 92.9 | -92.9 | | -163.2 | 0.0 |
| 2 | | | | 1.343 | 1.470 | 1.343 | | | | | | | | -178.5 | 37.8 |
| 3 | 1.201 | 1.580 | 1.580 | 1.512 | 1.352 | 1.512 | | 133.0 | 133.0 | | 124.6 | -124.6 | | 160.9 | 0.0 |
| 3TS | 1.170 | 1.986 | 1.986 | 1.451 | 1.366 | 1.451 | | 140.4 | 140.4 | | 122.4 | -122.4 | | 166.4 | 0.0 |
| 4 | | | | 1.397 | 1.397 | 1.397 | | | | | | | | 180.0 | 0.0 |
| 5 | 1.202 | 1.404 | 1.552 | 1.383 | 1.349 | 1.456 | 1.223 | 123.0 | 130.3 | 132.2 | 180.0 | 180.0 | 180.0 | | 0.0 |
| 5TS | 1.154 | 2.108 | 1.947 | 1.256 | 1.424 | 1.369 | 1.193 | 114.6 | 153.3 | 149.4 | 180.0 | 180.0 | 180.0 | | 0.0 |
| 6 | | | | 1.230 | 1.460 | 1.337 | 1.171 | | | 178.8 | | | | | 0.0 |
| 7 | 1.219 | 1.388 | 1.563 | 1.396 | 1.355 | 1.463 | 1.225 | 127.6 | 128.3 | 131.0 | 180.0 | 180.0 | 180.0 | 180.0 | 0.0 |
| 7TS | 1.157 | 2.134 | 1.988 | 1.303 | 1.428 | 1.366 | 1.195 | 118.7 | 150.9 | 149.9 | 167.7 | -178.0 | 174.5 | 172.6 | -13.4 |
| 8 | | | | 1.290 | 1.457 | 1.334 | 1.174 | | | 180.0 | | | | 180.0 | 0.0 |
| 9 | 1.213 | 1.471 | 1.471 ^d | 1.569 | | | | 147.8 | | | 0.0 | | | | |
| 9TS | 1.192 | 1.465 | 2.074 ^d | 1.461 | | | | 166.9 | | | 0.0 | | | | |
| 11 | 1.207 | 1.394 | 1.524 | 1.393 | 1.337 | 1.496 | | 122.0 | 129.9 | | 180.0 | 180.0 | | | 0.0 |
| 11TS | 1.166 | 2.261 | 1.769 | 1.268 | 1.415 | 1.417 | | 120.7 | 135.6 | | -85.7 | 71.3 | | | -1.2 |
| 12 | | | | 1.228 | 1.482 | 1.341 | | | | | | | | | 0.0 |
| 13 | 1.220 | 1.523 | 1.549 | 1.507 | 1.350 | 1.472 | 1.225 | 127.9 | 124.9 | 129.5 | 180.0 | 180.0 | 180.0 | 119.3 | 0.0 |
| 13TS | 1.160 | 2.449 | 1.868 | 1.370 | 1.422 | 1.384 | 1.202 | 129.5 | 140.8 | 147.6 | 116.3 | 116.3 | 163.0 | 169.6 | -30.2 |
| 14 | | | | 1.344 | 1.467 | 1.329 | 1.180 | | | 179.2 | | | | 177.2 | -22.0 |
| 15 | 1.209 | 1.400 | 1.495 | 1.387 | 1.347 | 1.451 | 1.345 | 122.3 | 130.9 | 132.5 | 180.0 | 180.0 | 180.0 | | 0.0 |
| 15TS | 1.160 | 2.154 | 1.964 | 1.260 | 1.422 | 1.365 | 1.333 | 119.7 | 136.0 | 148.2 | -169.6 | 152.6 | 146.8 | | -7.5 |
| 16 | | | | 1.226 | 1.483 | 1.321 | 1.309 | | | 179.5 | | | | | 0.0 |

^a Atom numbering as in Figure 3. At the MP2/6-31G* level, the C–O distance in carbon monoxide is 1.151 Å and the C–C distance in ethene is 1.336 Å. ^b Reference 7. ^c These structures have also been reported at the MP2(FU)/6-31G* level. Reference 27c. ^d C₂–C₄ distance.

Table 2. Lowest or Imaginary Frequencies, Carbonyl and Ketene Frequencies, Dipole Moments, and Symmetries of All Structures Optimized at the MP2(FC)/6-31G* Level Unless Otherwise Indicated with Experimental Values in Parentheses

| structure | point group | low (imag) freq ^a | C=O freq ^a | dipole moment ^b |
|--------------------------------|-----------------|------------------------------|------------------------------|---------------------------------|
| 1 | C _{2v} | 70.0 | 1815.5 (1774) ^c | 3.29 (2.79 ± 0.03) ^d |
| 1TS | C _s | 505.3i | 1993.3 | 1.69 |
| 2 | C ₂ | 186.0 | | 0.10 |
| 3 | C _{2v} | <i>e</i> | <i>e</i> (1846) ^f | 3.29 |
| 3TS | C _{2v} | <i>e</i> | | 1.80 |
| 4 | D _{6h} | 379.5 | | 0.0 |
| 5 | C _s | 149.0 | 1787.9, 1879.1 | 5.44 |
| 5TS | C _s | 351.5i | 2055.9, 2094.4 | 2.54 |
| 6 | C _s | 144.9 | 1740.3, 2228.3 | 3.99 |
| 7 | C _s | 99.5 | 1776.2, 1836.8 | 6.81 |
| planar 7TS ^g | C _s | 93.2i, 362.9i | | |
| 7TS | C ₁ | 347.7i | 2059.7, 2074.3 | 4.07 |
| 8 | C _s | 150.3 | 1680.7, 2227.7 | 3.58 |
| 9 | C _{2v} | 316.5 | 1933.6 (1813) ^h | 3.39 (2.67 ± 0.1) ⁱ |
| 9TS | C _s | 708.8i | 2012.7 | 2.37 |
| 10 | D _{2h} | 849.6 | | 0.0 |
| 11 | C _s | 161.5 | 1886.8 (1834) ^j | 4.53 |
| 11TS | C ₁ | 507.1i | 1982.7 | 3.14 |
| 12 | C _s | 165.3 | 1767.9 | 3.12 |
| 13 | C _s | 95.3 | 1776.0, 1805.3 | 6.04 |
| 13TS | C ₁ | 384.3i | 1997.3, 2016.6 | 3.11 |
| 14 | C _s | 89.1 | 2215.0 | 1.87 |
| 15 | C _s | 154.3 | 1872.1 | 4.58 |
| 15TS | C ₁ | 572.0i | 2034.4 | 3.64 |
| 16 | C _s | 146.7 | 1759.3 | 3.19 |
| carbon monoxide | C _{∞v} | | 2119.0 | 0.44 |

^a In cm⁻¹, unscaled. ^b In D. Based on the RHF/6-31G* wavefunction at the MP2/6-31G* geometry. ^c Reference 27a. ^d Reference 7. ^e Not calculated. ^f Reference 50. ^g This saddle point was constrained to C_s symmetry. ^h Reference 52a. ⁱ Reference 55. ^j Reference 61.

motion away from the butadiene. Although this is the so-called linear pathway (*vide supra*), the departure of the CO is not at all linear.

The barrier to thermal decarbonylation of **1** is calculated to be 49.0 kcal/mol, which is in good agreement with the experimental activation energy of 51.3 ± 0.2 kcal/mol⁴⁷ or 46.4 ± 2.4 kcal/mol⁴⁸ and that previously calculated by Quirante, 50.28 kcal/mol.^{27c} The overall reaction is calculated to be 18.9 kcal/mol endothermic, which compares favorably with the endothermicity of 20 ± 2 kcal/mol estimated by Simpson *et al.*^{28a} The agreement of this MP4(SDTQ)/D95** energy with Simpson's estimate is closer than that calculated by Quirante at the MP2(FU)/6-31G* level, 26.16 kcal/mol.

Two allowed pathways were predicted by Woodward and Hoffmann for the decarbonylation of **1**, the so-called linear-suprafacial (while disrotatory on butadiene, the departure of CO is not along the molecular axis) and the nonlinear-antarafacial (conrotatory) ones.² The calculated transition state is consistent with the former; a search for a nonlinear pathway was unsuccessful. More importantly, this calculated "linear" pathway (**1TS**) is consistent with all the available experimental data, as discussed below.

Product analyses can elucidate the stereochemistry of the diene portion. The facile decarbonylations of norbornenone ($\Delta G^\ddagger = 31$ kcal/mol)⁴⁹ and of norbornadienone (**3**, $\Delta G^\ddagger = 15$ kcal/mol)^{42,50} are both constrained to disrotatory pathways. Only recently have we demonstrated that in an unconstrained system, *cis*-2,5-dimethyl-3-cyclopentenone, thermal decarbonylation occurs exclusively via the disrotatory pathway.^{27f}

Information on the mode of departure of the CO is quickly lost after decarbonylation; however, elegant pump-probe studies have determined the vibrational, rotational, and translational energy distributions in the CO immediately following gas-phase

(47) Dolbier, W. R., Jr.; Frey, H. M. *J. Chem. Soc., Perkin Trans. 2* **1974**, 1674.

(48) Buxton, J. P.; Simpson, C. J. S. M. *Chem. Phys.* **1986**, *105*, 307–316.

(49) (a) Clarke, S. C.; Johnson, B. L. *Tetrahedron* **1971**, *25*, 3555–3561. (b) Battiste, M. A.; Visnick, M. *Tetrahedron Lett.* **1978**, 4771–4774.

(50) (a) LeBlanc, B. F.; Sheridan, R. S. *J. Am. Chem. Soc.* **1985**, *107*, 4554–4555. (b) Birney, D. M.; Berson, J. A. *J. Am. Chem. Soc.* **1985**, *107*, 4553–4554.

Table 3. Relative Energies (kcal/mol) of All Structures, Optimized at the MP2/6-31G* Level Unless Otherwise Indicated

| structure | RHF 6-31G* ^a | MP2 6-31G* ^b | RHF D95** | MP2 D95** ^b | MP3 D95** ^b | MP4(SDQ) D95** ^b | MP4(SDTQ) D95** ^b | MP4(SDTQ) + ZPE ^c |
|------------------------|----------------------------|----------------------------|--------------|---------------------------|---------------------------|--------------------------------|---------------------------------|---------------------------------|
| 1 | 0.0 | 0.0 | 0.0 | 0.0 | 0.0 | 0.0 | 0.0 | 0.0 |
| 1TS | 68.4 | 52.0 | 69.5 | 51.8 | 59.9 | 58.5 | 51.5 | 49.0 |
| 2 | 16.0 | 25.8 | 18.9 | 27.3 | 26.8 | 23.6 | 23.6 | 18.9 |
| 3 | <i>d</i> | 0.0 | 0.0 | 0.0 | 0.0 | 0.0 | 0.0 | 0.0 |
| 3TS | <i>d</i> | 13.7 | 25.9 | 14.0 | 21.1 | 20.7 | 15.2 | <i>e</i> |
| 4 | <i>d</i> | -33.9 | -49.7 | -31.5 | -33.1 | -33.3 | -32.5 | <i>e</i> |
| 5 | 0.0 | 0.0 | 0.0 | 0.0 | 0.0 | 0.0 | 0.0 | 0.0 |
| 5TS | 33.3 | 25.0 | 34.9 | 25.4 | 35.2 | 27.9 | 21.9 | 19.2 |
| 6 | 0.5 | 10.5 | 4.0 | 11.6 | 14.8 | 9.1 | 8.9 | 4.5 |
| 7 | 0.0 | 0.0 | 0.0 | 0.0 | 0.0 | 0.0 | 0.0 | 0.0 |
| 7TS^f | 48.4 | 40.9 | 50.4 | 41.4 | 48.5 | 42.9 | 37.5 | 34.5 |
| 7TS | <i>g</i> | 40.7 | 51.1 | 41.3 | 48.5 | 43.2 | 37.6 | 34.8 |
| 8 | 15.3 | 25.7 | 20.3 | 27.2 | 28.0 | 23.3 | 23.4 | 19.0 |
| 9 | 0.0 | 0.0 | 0.0 | 0.0 | 0.0 | 0.0 | 0.0 | 0.0 |
| 9TS | 53.1 | 43.0 | 54.1 | 40.8 | 45.6 | 43.8 | 39.3 | 37.5 |
| 10 | -27.3 | -14.7 | -25.8 | -15.2 | -16.5 | -19.5 | -19.0 | -22.4 |
| 11 | 0.0 | 0.0 | 0.0 | 0.0 | 0.0 | 0.0 | 0.0 | 0.0 |
| 11TS | 64.5 | 53.9 | 71.1 | 54.1 | 63.4 | 58.4 | 51.3 | 48.6 |
| 12 | 12.8 | 21.4 | 12.4 | 22.3 | 22.3 | 17.6 | 18.1 | 13.3 |
| 13 | 0.0 | 0.0 | 0.0 | 0.0 | 0.0 | 0.0 | 0.0 | 0.0 |
| 13TS | 58.8 | 41.7 | 59.5 | 41.9 | 51.8 | 48.3 | 40.6 | 37.4 |
| 14 | 14.9 | 24.1 | 18.4 | 25.4 | 27.0 | 22.9 | 22.4 | 17.6 |
| 15 | 0.0 | 0.0 | 0.0 | 0.0 | 0.0 | 0.0 | 0.0 | 0.0 |
| 15TS | 69.9 | 60.2 | 73.4 | 60.7 | 67.6 | 62.5 | 57.0 | 53.7 |
| 16 | 24.7 | 37.1 | 27.8 | 38.9 | 37.8 | 32.9 | 34.2 | 29.2 |

^a RHF/6-31G* geometry optimization. ^b Frozen core approximation. ^c Scaled by 0.9646, ref 35. ^d See ref 42. ^e No frequency calculation was done. ^f Constrained to C_s symmetry. ^g The transition state was planar at the RHF/6-31G* level.

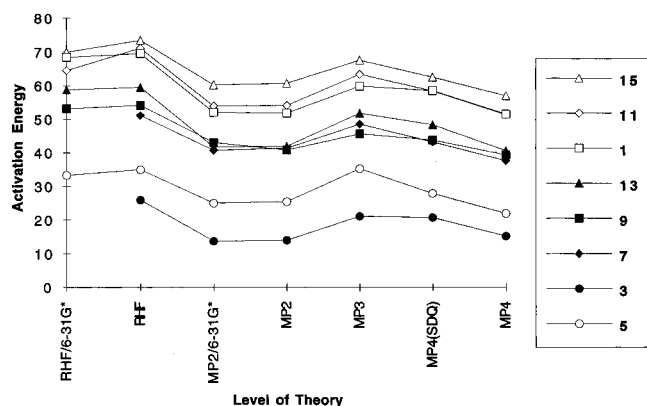


Figure 4. Plot of activation energies (in kcal/mol) for decarboxylations, as calculated at various levels of theory, from Table 4. The D95** basis set was used unless otherwise noted.

dissociation of **1**.^{28b,c} The product CO had less vibrational energy than statistically predicted. The rotational temperatures (3500 ± 140 , $\nu = 0$; 7500 ± 400 K, $\nu = 1$) are much higher than the vibrational one (1750 K), and the rotation vector is perpendicular to the velocity vector. These results were interpreted in terms of a concerted fragmentation,^{28b} with both C–C bonds breaking simultaneously as the CO bends out of the molecular plane. These results are consistent with the geometry of the calculated transition state.

These authors assume that the fragmentation occurs from the ground electronic state,^{28b,c} although much earlier work has demonstrated that in benzene solution and in the gas-phase photolysis of **1**, photochemical decarboxylation occurs only from the $n-\pi^*$ triplet.⁵¹ A correlation diagram shows that the fragmentation from the lowest $n-\pi^*$ singlet is allowed via the

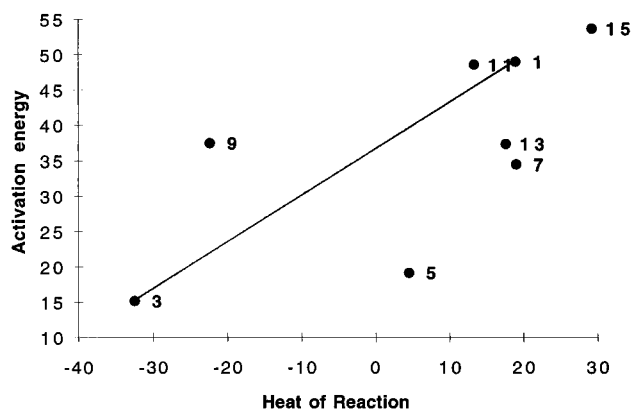


Figure 5. Plot of calculated activation energies versus calculated heats of reaction (kcal/mol, MP4/D95** + ZPE energies, except for **3**, which lacks the ZPE correction). The solid line simply connects the data for **1** and **3**, which are the two carbocyclic allowed pericyclic reactions and have similar orbital topologies.

same linear-suprafacial pathway as is the thermal fragmentation.⁸ Formation of rotationally hot CO in $\nu = 1$ could be rationalized if it were formed in conjunction with ground state butadiene, while the CO in $\nu = 0$ was formed in conjunction with excited state triplet butadiene. The latter reaction would be a less exothermic reaction and could lead to rotationally and vibrationally colder CO.

In shock-tube experiments by Simpson *et al.*, there is no question that fragmentation occurs from the ground state.^{28a} Although the vibrational and rotational states were not completely resolved, it was clear that the CO initially produced is vibrationally cooler than the butadiene, again reflecting a nonstatistical distribution of vibrational energy. These authors suggest that this energy partitioning indicates that at the transition state, the CO bond length is closer to that of the product CO than to that of the carbonyl in **1**. This qualitative prediction is borne out in the calculated geometries. The C=O

(51) (a) Nakamura, K.; Koda, S.; Akita, K. *Bull. Chem. Soc. Jpn.* **1978**, *51*, 1665. (b) Darling, T. R.; Pouliquen, J.; Turro, N. J. *J. Am. Chem. Soc.* **1974**, *96*, 1247.

distance in **1** shortens by 0.054 Å at the transition state **1TS**, while this distance only shortens by an additional 0.016 Å in the product CO. The nature of the shock tube experiment precludes measurement of the nascent rotational excitation of the CO; Simpson *et al.* also suggest that the high rotational excitation of photochemically produced CO indicates a non-symmetrical bond cleavage.^{28a} However, as discussed above, the rotational excitation is indeed consistent with the calculated synchronous transition state. The weight of the experimental evidence supports the “linear” disrotatory pathway (Figure 1A) as proposed by Woodward and Hoffmann² and as calculated here and by others.^{27c,e}

There is one further detail of the calculated geometry of **1TS** to be discussed. At the transition structure, the CO has tipped significantly over the butadiene, as seen in Figure 3. This geometry minimizes the repulsion between the developing lone pair on the carbon monoxide and the electron rich π -system of the butadiene (see Figure 1A). A similar effect is seen in several of the other transition structures as discussed below.

Bicyclo[2.2.1]hepta-2,5-dien-7-one (3). The decarbonylation of **3** was of interest in comparison to that of **1**, as it is also a [4 + 1] pericyclic reaction, but it is substantially exothermic and correspondingly has a much lower barrier.^{42,46,50} Thus the decarbonylations of **1** and **3** provide a baseline correlation for an allowed pericyclic cheletropic decarbonylation with an all-carbon framework. One would expect that a reaction that has a higher barrier than expected in Figure 5 for its exothermicity lacks the energy of concert, while for a reaction with a lower than expected barrier, there is some additional factor that makes the reaction easier. One of us has previously reported RHF/6-31G* and MP2(FU)/4-31G calculations on the decarbonylation of **3**.⁴⁶ This work extends the calculations to the MP4-(SDTQ)/D95** level. The calculated activation energy of 15.2 kcal/mol is in agreement with the observed E_a of 15.2 kcal/mol.⁵⁰ The structures of **3** and of the transition state **3TS** were similar to those discussed previously.⁴⁶ The C_{2v} geometry of this transition state corresponds to the linear-suprafacial pathway.

Cyclopropanone (9). Although cyclopropanone (**9**) itself will polymerize if heated,⁵² other derivatives will thermally decarbonylate.⁵³ This decarbonylation has been examined theoretically by *ab initio* calculations,⁵⁴ although these studies were limited by the use of the STO-3G basis set. The calculated transition structures agree qualitatively with the nonlinear pathway predicted by Woodward and Hoffmann. There is good agreement between the microwave structure⁵⁵ and that calculated at the MP2/6-31G* level for **9**.⁵⁶

The geometry of the transition structure **9TS** calculated here at the MP2/6-31G* level (Figure 3) is in many, but not all, respects similar to those calculated at lower levels of theory. The departing CO remains in the molecular plane, but the pathway is nonlinear in that the CO bends away from the C2 axis of **9**. The pathway is very asynchronous; one of the breaking bonds is 0.609 Å longer than the other in **9TS**. Interestingly, the shorter of the breaking bonds in **9TS** is actually slightly longer (by 0.006 Å) in **9** than in **9TS**!

(52) (a) Turro, N. J.; Hammond, W. B. *J. Am. Chem. Soc.* **1966**, *88*, 3672–3673. (b) Rodriguez, H. J.; Chang, J.-C.; Thomas, T. F. *J. Am. Chem. Soc.* **1976**, *98*, 2027–2034.

(53) Pazos, J. F.; Pacifici, J. G.; Pierson, G. O.; Sclove, P. B.; Greene, F. D. *J. Org. Chem.* **1974**, *39*, 1990.

(54) (a) Yamabe, S.; Minato, T.; Osamura, Y. *J. Am. Chem. Soc.* **1979**, *101*, 4525–4531. (b) Sevin, A.; Fazilleau, E.; Chaquin, P. *Tetrahedron* **1981**, *37*, 3831–3837.

(55) Pochan, J. M.; Baldwin, J. E.; Flygare, W. H. *J. Am. Chem. Soc.* **1969**, *91*, 1896–1898.

(56) Staley, S. W.; Norden, T. D.; Taylor, W. H.; Harmony, M. D. *J. Am. Chem. Soc.* **1987**, *109*, 7641–7647.

The oxygen of the CO is rotated over the ethene in **9TS**.^{54a} As discussed above, the description of the orbital interactions first proposed by Woodward and Hoffmann is not entirely satisfactory. The calculated geometry and charges suggest an alternative as shown in Figure 2C. In this model, there is primarily donation from the ethene π -HOMO into the CO π^* -LUMO, thus developing the partial positive charge on C₄. This partial positive charge cannot be stabilized by orbital overlap, which would lead to an antiaromatic system, but is stabilized by an electrostatic attraction from the partially negative oxygen. This holds the oxygen over the ethene even as the CO departs in **9TS**.

The calculated barrier for the decarbonylation of **9** is 37 kcal/mol. This is more reasonable than the barriers of 15 kcal/mol^{54b} or 80 kcal/mol^{54a} previously calculated, and it is high enough to rationalize the observed preference for polymerization. Although there are other allowed pericyclic reactions with barriers of similar or greater magnitude, Figure 5 shows that this barrier is substantially higher than would be expected for an allowed cheletropic decarbonylation of comparable exothermicity. The “energy of concert”, if it exists, is smaller than that for **1** and **3**. For this and the other reasons discussed above, the most reasonable conclusion is that this prototypical “non-linear” decarbonylation, although formally orbital symmetry allowed, is in a sense “effectively forbidden”.

2,3-Furandione (5). The thermal and photochemical decarbonylation of furandione (**5**) has been useful for the generation and matrix IR identification of substituted acetylketenes since the CO byproduct has a single IR absorption.^{29,33} The thermal reactions proceed smoothly under flash vacuum pyrolysis (FVP) conditions above approximately 200 to 300 °C. However, the activation energy has not been determined.

The calculated transition structure (**5TS**) for the decarbonylation of **5** is shown in Figure 3. The striking contrast between the planarity of this structure and the out-of-plane motion of the CO in **1TS** and **3TS** is a consequence of the pseudopericyclic orbital topology of **5TS** (Figure 1, *vide supra*). The reaction is concerted and is more synchronous than the analogs **11** and **13**. The C₂–O₃ bond has lengthened 0.704 Å from **5** to **5TS**, while the C₂–C₆ bond has only lengthened by 0.395 Å. It is perhaps surprising that the ester C–O bond is more broken at the transition structure **5TS**, rather than the single bond between the two carbonyl groups; usually esters are stabilized and α -dicarbonyl compounds are destabilized.⁵⁷ However, the nearly linear O₁–C₂–C₆ geometry (153.3°) suggests that it is more appropriate to consider the reverse reaction, the interaction of CO with formylketene (**6**), in which donation of the CO lone pair to the in-plane ketene HOMO is the dominant interaction, and leads to the nearly linear geometry. There would be little back-bonding into the CO π^* , and indeed there is a net transfer of +0.107 esu charge from the CO to the ketene in **5TS** (see Supporting Information).

Experimental measurement of the energy distributions in the product carbon monoxide should provide an interesting contrast to **1**. Comparison of the optimized geometries of **5** and **5TS** in Figure 6 suggests that there is very little rotational motion imparted to the CO in the transition structure. Thus there should be much lower rotational excitation in the carbon monoxide formed from **5** than in that formed from **1**. Furthermore, Simpson's theory predicts very little vibrational excitation in

(57) However, note that a substituted derivative of **7** is subject to nucleophilic attack at the amide carbonyl.⁵⁸

(58) Aliev, Z. G.; Maslivets, A. N.; Simonchik, O. L.; Konyukhova, T. G.; Andreichikov, Y. S.; Atovmian, L. O. *Russ. Chem. Bull.* **1995**, *44*, 1496–1498.

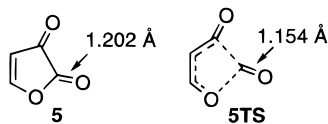


Figure 6. Comparison of MP2/6-31G* optimized geometries of **5** and **5TS**. The structures are drawn to the same scale.

the carbon monoxide, as the CO distance is only 0.003 Å longer in the transition state **5TS** (1.154 Å) than in carbon monoxide.^{28a}

The calculated barrier for the decarbonylation of **5** is 19.2 kcal/mol. Depending on the activation entropy, this might be somewhat lower than expected for a system that is stable at room temperature but readily undergoes decarbonylation at elevated temperatures. The reaction is calculated to be 4.5-kcal/mol endothermic. Examination of Figure 5 and comparison with **3** are instructive. The decarbonylation of **3** is calculated to be 32.5-kcal/mol exothermic, yet the calculated barrier is only 15.2 kcal/mol (MP4(SDTQ)/D95**//MP2/6-31G*). Thus, there is a much greater driving force for the decarbonylation of **3** than of **5** (37.0-kcal/mol difference), yet this translates into only a 4.0 kcal/mol lower calculated barrier for **3** versus **5**. The relative ease of decarbonylation of **5** is therefore attributable to the pseudopericyclic nature of the transition state, in which the lack of cyclic orbital overlap minimizes electron–electron repulsion.

2,3-Pyrroledione (7). Decarbonylations of pyrrolediones have been used to generate a variety of imidoylketenes, both as transient intermediates and for matrix isolation IR studies.³⁰ This reaction, like that of **5**, proceeds readily, either under static pyrolysis or FVP conditions. The two systems (**5** and **7**) are isoelectronic and thus **7TS** was anticipated to also be a planar, pseudopericyclic transition structure. This expectation was not entirely borne out; in the transition structure **7TS**, the CO is slightly out of plane (Figure 3). However, the planar, second-order saddle point is only 0.3 kcal/mol above **7TS**. Given such a small difference in energy between the two pathways, it is inappropriate to attach great significance to this difference; however, it is consistent with a rehybridization of N₃ from sp² toward sp³ to accommodate the calculated increase in negative charge on N₃ in **7TS** (see Supporting Information). In other respects, the geometry of the transition structure is quite similar to that found for **5TS**. It is concerted and asynchronous, with the C₂–N₃ bond more broken than the C₂–C₆ bond (0.746- and 0.425-Å extensions, respectively). The O₁–C₂–C₆ angle is 150.9°, again suggesting that the structure may be viewed primarily as the interaction of a CO lone pair with the imidoylketene.

The calculated barrier for the decarbonylation of **7** (34.5 kcal/mol) is substantially higher than that for **5** (19.2 kcal/mol). This reflects the higher endothermicity for the fragmentation of **7** as opposed to **5** (19 and 4.5 kcal/mol, respectively). Two factors contribute to this. Electron-withdrawing groups stabilize ketenes and carbonyls are more electron withdrawing than imines, thus **6** is more stabilized than **8**. Also, resonance in amides is stronger than in esters, thus **7** is more stabilized than **5**.

A direct comparison of barrier heights for **5** and **7** is not possible. However, pyrrolediones are observed to decarbonylate at temperatures ranging from 160 to 185 °C in static systems or above 300 °C under FVP conditions.³⁰ This compares to temperatures of 110 °C in static systems or 200–250 °C under FVP conditions required for derivatives of **5**.^{29,33} Thus the calculated barriers are at least qualitatively consistent.

3H-Furan-2-one (11), 3-Cyclopentene-1,2-dione (13), and 3-Methylene-3H-furan-2-one (15). These three compounds were included in this study because they contain some, but not

all, of the factors that contribute to the planar, pseudopericyclic orbital topology found in **5TS** and **7TS** (see Figure 1). In **11**, there are only orthogonal orbitals on the furan oxygen (O₁), in **13**, there are only orthogonal orbitals on what will become the ketene carbon and oxygen (C₆ and O₇), and in **15**, although there are orthogonal orbitals on both O₁ and C₆, this structure lacks the orthogonal orbitals on C₇ that are present on the oxygens (O₇) in the ketenes **6** and **8**.

There have been no previous *ab initio* studies on the decarbonylation of **11**.⁵⁹ The geometry of the concerted transition structure **11TS** for the decarbonylation of **11** is remarkably similar to that (**1TS**) of the decarbonylation of **1**. The CO has moved significantly above the molecular plane, and the oxygen is tipped back over the butadiene (*vide supra*). Despite the potential for an orbital orthogonality on O₃, the geometry of **11TS** indicates that this is a pericyclic reaction. The one significant geometrical difference between **11TS** and **1TS** is with respect to asynchronicity. While **1TS** is synchronous, by virtue of its symmetry, **11TS** is the most asynchronous of the five-membered-ring decarbonylations calculated here. As was the case for **5TS** and **7TS**, the sense of asynchronicity suggests that 1,4-nucleophilic addition of CO to the electron-deficient C₆ of acrolein leads the reverse reaction (Supporting Information). This primary interaction is not at a center which bears an orbital orthogonality.

This reaction has a high calculated activation energy of 48.6 kcal/mol, which is almost the same as that calculated for **1TS** (49.0 kcal/mol). Although **11** is a known compound, the experimental barrier height for its decarbonylation is not available for comparison.⁶¹ Both reactions also have similar calculated heats of reaction; decarbonylation of **11** is 13.3-kcal/mol endothermic, while that of **1** is 18.9-kcal/mol endothermic. The similarity of the reaction profiles for the two reactions also suggests that **11TS** is a pericyclic reaction. Indeed, Figure 5 suggests that the barrier is slightly higher than expected. Clearly this single orbital disconnection on O₃ in **11** is not sufficient to allow the reaction to be pseudopericyclic.⁶²

The decarbonylation of **13** provides a similar test as to whether the potential orbital orthogonality on the developing ketene carbon (C₆) is sufficient to allow the decarbonylation to be pseudopericyclic. Compound **13** is also a known compound,⁶⁴ and the decarbonylation of the benzo-fused derivative has been reported.⁴⁴ The calculated transition structure **13TS** is similar in geometry to both **1TS** and **11TS**. It is almost as asynchronous as **11TS**; again nucleophilic addition of carbon monoxide to the electron-deficient C₆ (Supporting Information) can be considered to lead the reverse reaction. Consistent with this, the O₁–C₂–C₆ angle of 140.8° is quite obtuse. In contrast to **11TS**, the strongest bonding in **13TS** occurs at the site of the orbital orthogonality. The CO in **13TS** has moved out of the molecular plane of **13**, but not as much as in **1TS** or **11TS**,

(59) A previous MINDO/3 study of the thermolysis of **11** reported a stepwise pathway.⁶⁰ For allowed pericyclic reactions, such pathways usually do not persist in higher level *ab initio* calculations,¹¹ and the results reported here are no exception.

(60) Arenas, J. F.; Quirante, J. J.; Ramirez, F. J. *J. Mol. Struct. (Theochem)* **1989**, *183*, 143–150.

(61) Bierbach, A.; Barnes, I.; Becker, K.; Wiesen, E. *Environ. Sci. Technol.* **1994**, *28*, 715–729.

(62) This is consistent with results of calculations on hetero-Diels–Alder reactions of acrolein, in which there was no tendency toward planar, pseudopericyclic transition structures.⁶³

(63) (a) Loncharich, R. J.; Brown, F. K.; Houk, K. N. *J. Org. Chem.* **1989**, *54*, 1129–1134. (b) Birney, D. M.; Houk, K. N. *J. Am. Chem. Soc.* **1990**, *112*, 4127–4133. (c) Yamabe, S.; Kawajiri, S.; Minato, T.; Machiguchi, T. *J. Org. Chem.* **1993**, *58*, 1122–1127.

(64) (a) Ralph, J.; Hatfield, R. D. *J. Agric. Food Chem.* **1991**, *39*, 1426–1437. (b) Quinkert, G.; Grosso, M. d.; Bucher, A.; Bauch, M.; Doring, W.; Bats, J. W.; Durner, G. *Tetrahedron Lett.* **1992**, *33*, 3617–3620.

nor is it tipped over the rest of the molecule. These factors suggests that there is some pseudopericyclic character to the reaction.

The calculated barrier height for the decarbonylation of **13** is 37.4 kcal/mol. This is substantially below that of **1** and **11** (49.0 kcal/mol and 48.6 kcal/mol, respectively), although this reaction is approximately as endothermic (17.6 kcal/mol) as either of the other two pericyclic reactions (18.9 and 13.3 kcal/mol for **1** and **11**, respectively). The lower activation energy would again be consistent with some pseudopericyclic character in **13TS**. In this case, a single orbital orthogonality at the ketene, where the strongest bonding occurs between the two fragments in the transition structure, leads to the low barrier associated with pseudopericyclic reactions.

Decarbonylations of substituted derivatives of **15** are known.⁶⁵ In **15** there are potentially orthogonal orbitals at both O₃ and C₆. Although there must be some twisting of the terminal methylene at C₇, the calculated transition structure (**15TS**) for this decarbonylation is more planar than **1TS**, **11TS**, or **13TS**. This implies more of a pseudopericyclic contribution to **15TS**. This transition structure is much less asynchronous than **11TS**, or **13TS**, and is even slightly more synchronous than **5TS**.

Decarbonylation of **15** is 29.2 kcal/mol endothermic, 11.6 kcal/mol more endothermic than **13**, and the most endothermic of the reactions examined here. This reflects, in large measure, the relative instability of formylallene (**16**), which is calculated here to be 13.0 kcal/mol less stable than the isomeric vinylketene (**14**).⁶⁶ It is not surprising, then, that it also has the highest barrier (53.7 kcal/mol). It is not obvious from Figure 5 whether or not there is some energetic benefit from the pseudopericyclic nature of this transition state. If there is, it must be small, however, for the barrier for decarbonylation of **15** is 16.3 kcal/mol higher than of **13**, which is more than the difference in the endothermicities. This is due in part to a poor match between electrophilic and nucleophilic sites (Supporting Information) in the two fragments, a factor that has been shown to raise barrier heights barrier heights in other pseudopericyclic systems.^{12c} There does not appear to be a significant "allene effect" as found in some sigmatropic rearrangements.⁶⁸

Conclusions

Transition structures for eight cheletropic decarbonylations were located at the MP2/6-31G* level. Relative energies of these and of reactants and products were obtained at the MP4-(SDTQ)/D95** + ZPE level. The energetics and geometry of the out-of-plane, "linear" pericyclic transition structure (**1TS**) for the decarbonylation of **1** are consistent with all the available experimental evidence. Together with the decarbonylation of **3**, this provides a baseline for considerations of the energetics of orbital symmetry allowed pericyclic decarbonylations. By

(65) Berstermann, H.-M.; Harder, R.; Winter, H.-W.; Wentrup, C. *Angew. Chem., Int. Ed. Engl.* **1980**, *19*, 564–565.

(66) Compounds **14** and **16** have also been studied by others.⁶⁷

(67) (a) Gong, L.; McAllister, M. A.; Tidwell, T. T. *J. Am. Chem. Soc.* **1991**, *113*, 6021–6028. (b) Wong, M. W.; Wentrup, C. *J. Org. Chem.* **1994**, *59*, 5279–5285.

(68) Jensen, F. *J. Am. Chem. Soc.* **1995**, *117*, 7487–7492.

the criterion of the Hammond postulate, the decarbonylation of cyclopropanone (**9**) has a significantly higher barrier than expected for an exothermic reaction. Thus, although it is formally orbital symmetry allowed, because it lacks an energetic benefit of concert, it should be considered to be "effectively forbidden".

In contrast to **1TS** and **3TS**, the transition structures **5TS** and **7TS** for decarbonylations of 2,3-furandione (**5**) and 2,3-pyrroledione (**7**) are planar, as a consequence of their pseudopericyclic orbital topology. Both **5TS** and **7TS** have two orbital disconnections. The planarity of these transition structures and the short C=O bonds predict that the carbon monoxide product should be formed rotationally and vibrationally cold. Furthermore, the pseudopericyclic orbital topology of these reactions, combined with favorable interactions between electrophilic and nucleophilic centers, results in barriers substantially lower than would be expected for pericyclic decarbonylations analogous to **1TS** and **3TS**.

The transition structure **11TS** has only a single orbital disconnection at an oxygen where the bonding between the two fragments is the weakest. It has a pericyclic geometry and a reaction profile similar to the decarbonylation of **1**. In contrast, transition structure **13TS**, which also has a single orbital disconnection, is pseudopericyclic. In this case, however, the strongest bonding between the fragments is at the disconnection. The geometry is close to planar, and the activation energy is much lower than expected for a pericyclic decarbonylation of similar exothermicity. Transition structure **15TS**, although it is also close to planar, lacks the lowered barrier of other pseudopericyclic reactions because there is a poor match between electrophilic and nucleophilic sites.

In those systems that have been studied, two orbital disconnections are sufficient to allow a reaction to be pseudopericyclic and to have an approximately planar transition structure. Orbital disconnections may occur at cumulene carbons as well as atoms with lone pairs. A single disconnection may, but will not always, lead to a (nearly) planar transition structure. However, in an asynchronous transition state, if the strongest bonding is at the disconnection, the reaction will have more pseudopericyclic character. Synergistic electrophile–nucleophile interactions lower barriers for pseudopericyclic reactions. In summary, when a pericyclic reaction has even one possible orbital disconnection (i.e., orthogonality) this may result in a pseudopericyclic transition structure. When there are two disconnections and favorable nucleophile/electrophile interactions, a low-barrier, pseudopericyclic pathway may be expected.

Acknowledgment. We thank Professors Curt Wentrup and E. Amitai Halevi for helpful discussions. The financial support of the Robert A. Welch Foundation is gratefully acknowledged.

Supporting Information Available: Cartesian coordinates and vibrational frequencies for all MP2/6-31G* optimized structures are available, as are tables of absolute energies and Mulliken charges (15 pages). See any current masthead page for ordering and Internet access instructions.

JA963551R